Appl. Phys. B 79, 799–803 (2004)
DOI: 10.1007/s00340-004-1659-3

Applied Physics B
Lasers and Optics

Rapid communication

M. HORSTJANN[1,*]
Y.A. BAKHIRKIN[1]
A.A. KOSTEREV[1]
R.F. CURL[1]
F.K. TITTEL[1,✉]
C.M. WONG[2]
C.J. HILL[2]
R.Q. YANG[2]

Formaldehyde sensor using interband cascade laser based quartz-enhanced photoacoustic spectroscopy

[1] Rice Quantum Institute, Rice University, Houston, TX 77251-1892, USA
[2] Jet Propulsion Laboratory, California Institute of Technology, 4800 Oak Grove Drive, Pasadena, CA 91109, USA

Received: 27 July 2004/Revised version: 14 September 2004

ABSTRACT A novel continuous-wave mid-infrared distributed feedback interband cascade laser was utilized to detect and quantify formaldehyde (H_2CO) using quartz-enhanced photoacoustic spectroscopy. The laser was operated at liquid-nitrogen temperatures and provided single-mode output powers of up to 12 mW at 3.53 μm (2832.5 cm^{-1}). The noise equivalent (1σ) detection sensitivity of the sensor was measured to be 2.2×10^{-8} cm^{-1} W $(Hz)^{-1/2}$ for H_2CO in ambient air, which corresponds to a detection limit of 0.6 parts in 10^6 by volume (ppmv) for a 10 s sensor time constant and 3.4 mW laser power delivered to the sensor module.

PACS 42.62.Fi; 72.50.+b

1 Introduction

The recent realization of distributed feedback (DFB) interband cascade lasers (ICLs) [1] has made it possible to access wavelengths between 3.0 and 4.5 μm [2, 3], a spectral region which has been difficult to cover with intraband quantum cascade lasers (QCLs). ICLs employ transitions between the conduction and valence bands as in bipolar diode lasers, but instead of losing an electron to the valence band it is recycled through interband tunneling into the conduction band of the next cascade stage. This is made possible with the type-II broken gap alignments in InAs/GaInSb quantum well structures. Because the conduction and valence bands have opposite dispersion curvatures, fast phonon scattering loss is circumvented in ICLs, which results in a more efficient operation with a low threshold current density. The emission wavelength of ICLs can be tailored in a wide spectral range, particularly on the shorter-wavelength side due to a large band offset between their constituent materials. Presently, continuous-wave (cw) operation of ICLs is obtained at cryogenic temperatures. However, there are no theoretical limitations preventing near-room-temperature operation. Such devices will be realized as technical issues are resolved. Continuous-wave operation with thermoelectric rather than cryogenic cooling has already been demonstrated for QCLs [4, 5].

The DFB-ICL used in this work emitted near 3.5 μm. This spectral region is important for various gas-sensing applications because it corresponds to a spectral range of the C–H stretch vibration of aldehydes (e.g. formaldehyde symmetric stretch) and alkanes (e.g methane). Formaldehyde (H_2CO) is of particular interest since it is a hazardous and carcinogenic substance, which is released from chemical binders present in numerous manufactured items and hence its presence in the environment cannot be avoided. The Occupational Safety and Health Administration (OSHA) has issued general industrial standards with an upper limit of 0.75 ppmv for long-term exposure (8 h time-weighted average) and 2 ppmv for short-term exposure (15 min) [6]. NASA has also established spacecraft maximum allowable concentration levels for crew exposure to H_2CO for extended periods of time [7]. H_2CO has been identified as a potential biomarker in breath analysis of human subjects. For example, in exhaled breath from breast cancer patients, concentration levels of 1.2 ppmv were observed [8]. Furthermore, H_2CO is an important and reactive component present in all regions of the atmosphere arising from the oxidation of biogenic and anthropogenic hydrocarbons. Tropospheric H_2CO concentration measurements provide a means of validating photochemical model predictions concerning hydrocarbon oxidation that are used to advance ozone chemistry [9, 10].

To quantify H_2CO concentrations, several different chemical [11, 12] and physical detection methods are used. Chemical analyzers, which employ coloration of a formaldehyde-sensitive reagent, are sensitive at ppbv levels but they suffer from cross-interference effects by other aldehydes and require long sampling times (i.e. minutes or more). To overcome these limitations, laser-based spectroscopic sensors have been developed. Several different tunable, cw laser sources have been employed to access H_2CO absorption lines, such as lead-salt lasers [9], difference-frequency generation (DFG) [13–15] sources, and CO overtone gas lasers [16]. Optical parametric oscillators (OPOs) [17, 18] and solid-state lasers [19] are also capable of addressing H_2CO absorption lines. The best

---

✉ Fax: +1-713-348-5686, E-mail: fkt@rice.edu
[*] *Present address:* Institut für Lasermedizin, Universitätsstraße 1, 40225 Düsseldorf, Germany

H_2CO detection sensitivity reported [9] (< 50 pptv) was achieved using lead salt diode laser based absorption spectroscopy in a multipass optical cell with an effective optical path length of 100 m.

Currently, ICLs provide optical output powers of ∼ 10 mW, a value which is expected to increase in the future. While the sensitivity of direct absorption spectroscopy does not fundamentally depend on laser power (neglecting the shot-noise limit), other approaches can make use of high spectroscopic source power to lower the detection limits. Photoacoustic spectroscopy (PAS) is one such approach. PAS sensitivity scales linearly with the available laser power. A novel modification of PAS, called quartz-enhanced PAS (QEPAS), also permits us to match the size of the laser source and the absorption detection module (ADM), both with a ∼ 1 cm characteristic linear dimension. In this work we report the development and performance characteristics of a formaldehyde sensor using a cw DFB-ICL and QEPAS. QEPAS is based on the photoacoustic signal build-up in a high-Q piezoelectrically active quartz crystal instead of a low-Q gas-filled resonator as in traditional PAS. It has advantages of a very small sample volume (∼ 1 mm^3) required for analysis and high immunity to ambient acoustic noise [20]. The sensitivity of QEPAS to a particular trace species is strongly dependent upon the V–T relaxation rate of this species in a certain host gas. If the rate is too slow, the thermal response giving rise to the detected pressure waves cannot follow the modulation frequency. A theoretical analysis of this rate is difficult and hence an experimental investigation is required to evaluate QEPAS sensitivity to specific chemical species. In this work we performed such studies for H_2CO detection in dry nitrogen, dry nitrogen with 5% of SF_6, and normal 50% humidity room air.

2 ICL parameters and H_2CO absorption-line selection

The ICL utilized in this work is able to operate continuously at temperatures of up to 170 K. The laser bias voltage is ∼ 7–8 V and the threshold current varies from 3 to 22 mA as the temperature changes from 78 K to 170 K. The laser frequency can be tuned continuously from 2833 cm^{-1} ($T = 78$ K) to 2816 cm^{-1} ($T = 170$ K) in a single-frequency mode by means of current and temperature tuning. The temperature tuning rate is 0.178 cm^{-1}/K. At a fixed heat-sink temperature of 78 K, the laser emits up to 12 mW and the output is tunable from 2831.8 cm^{-1} to 2833.7 cm^{-1} by current (see Fig. 1) with a tuning rate of 0.0327 cm^{-1}/mA. The low threshold current operation of ICLs requires a current source with relatively high resolution (an ILX Lightwave model LDX 3220 was used). The line width of a similar ICL operating at 3.3 µm was measured to be < 20 MHz [21].

With the available ICL operating at 78 K it is possible to access four significant formaldehyde absorption lines (see Fig. 2). For H_2CO measurements in ambient air at concentrations < 50 ppbv, a line at 2833.190 cm^{-1} (line no. 4) is favorable because it is free from interference by water and methane. However, this line was not selected because the ICL power at this frequency is ∼ 2 times smaller than the powers at the spectral positions of other available absorption lines. This results in a weaker QEPAS signal, because the QEPAS signal scales with excitation power. Line no. 1 at 2832.146 cm^{-1} is a superposition of two lines and provides a smaller QEPAS signal than the absorption line no. 2 at 2832.483 cm^{-1} selected for this study.

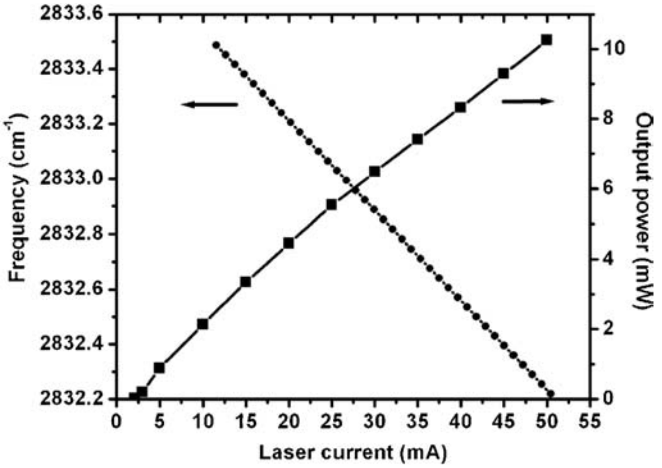

FIGURE 1 Dependence of the laser frequency and optical output power on the ICL current at $T = 78$ K. The frequency calibration was obtained using the H_2CO absorption spectrum and a 15-cm air-spaced etalon formed by two uncoated ZnSe surfaces

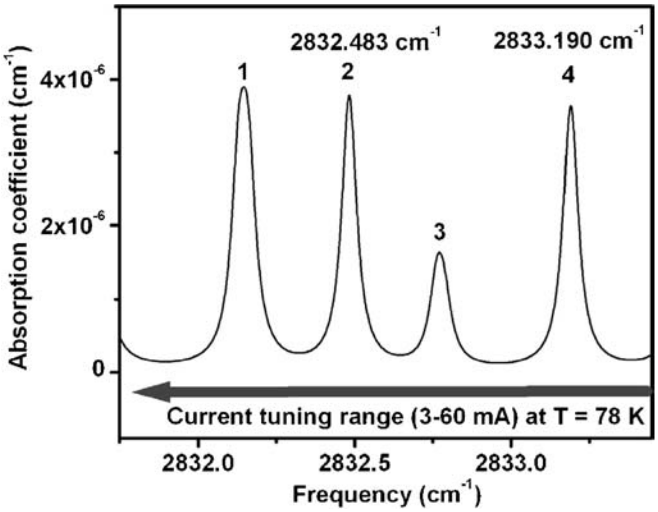

FIGURE 2 HITRAN 2000 simulation of four H_2CO absorption lines at a total pressure of 200 Torr and 1 ppmv concentration. The *arrow* indicates the ICL current-tuning range. Increasing current causes the frequency to decrease

Line no. 2 was accessed with an ICL drive current of 42 mA. The optimum H_2CO absorption line at 2831.642 cm^{-1} used in [9, 13–15] is also accessible with this ICL at heat-sink temperatures > 78 K.

3 Description of the ICL-based QEPAS sensor platform

The H_2CO sensor is depicted schematically in Fig. 3. The QEPAS ADM consisting of a crystal resonator/transducer and acoustic microresonator has been described in earlier publications [20, 22, 23]. Briefly, a watch tuning fork (TF) is used as the photoacoustic transducer. Two glass tubes (2.54 mm in length and 320-μm inner diameter) are arranged on both sides of the TF forming an acoustic microresonator, which enhances the QEPAS signal by a factor of ~ 10. The piezoelectric current generated by the excitation of the TF by photoacoustic wave action is converted to a voltage by a transimpedance amplifier (feedback resistor $= 10\,M\Omega$). The ADM is placed into a gas cell with a volume of $\sim 1\,cm^3$. The outer dimensions of the cell with electrical feedthroughs, pressure gauge, swage-lock fittings, and transimpedance amplifier mounted on the ISO-KF flange are $2.5'' \times 1.5'' \times 2.5''$.

The ICL is mounted inside a liquid nitrogen (LN_2) cooled cryostat (Cryo Industries, Inc.). The ICL radiation (wavelength modulated at half the TF frequency of $f \sim 32$ kHz) is focused into the ADM with a ZnSe lens (focal length 12.5 mm, 25-mm diameter). The QEPAS signal is subsequently demodulated by a lock-in amplifier (Stanford Research model SR830 DSP) at frequency f (second-harmonic detection) and processed by a laptop computer. A CaF_2 beam splitter directs 5% of the ICL beam through a short reference cell (5-cm long) filled with paraformaldehyde (which sublimes to H_2CO with a vapor pressure of 1.45 Torr at 300 K). A photodetector signal is demodulated by a second lock-in amplifier at the third harmonic of the $f/2$ reference and used as a feedback to lock the laser frequency to the H_2CO absorption line via a proportional adjustment of the ICL current offset.

A gas standard generator (Kin-Tek model 491M) based on a permeation tube was used to provide H_2CO concentrations ranging from 0.5 to 25 ppmv in a diluting gas (i.e. N_2 or air). The QEPAS cell pressure was maintained constant by means of a pressure controller (MKS Instruments type 659), which also measured the gas flow (fixed at 75 sccm for all measurements with a needle valve located after the QEPAS cell). Since formaldehyde is a sticky molecule with a high dipole moment (2.3 D), ultra-pure PFA (perfluoroalkoxy) tubing was employed in the gas-flow system. This type of tubing has a smooth interior surface, thereby reducing adsorption of H_2CO to the tubing walls. The QEPAS signal showed no dependence on the flow rate.

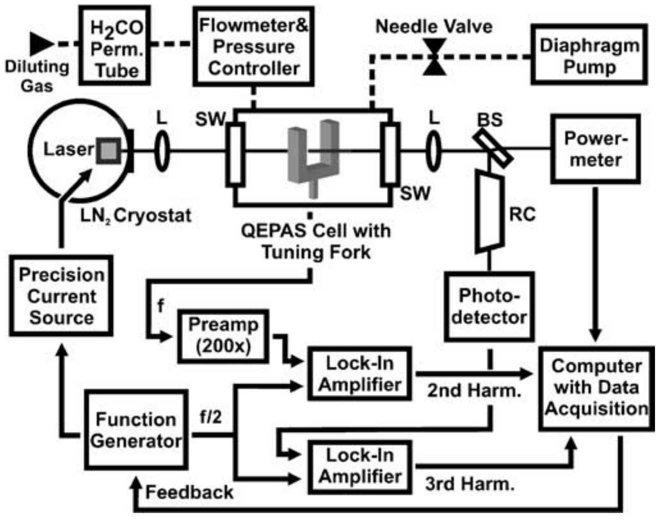

FIGURE 3 Schematic of ICL-based QEPAS H_2CO sensor architecture. L – lens, BS – beam splitter, RC – reference cell, SW – sapphire windows, Perm. – permeation, Preamp – preamplifier, Harm. – harmonic. The reference frequency supplied to both lock-in amplifiers from the function generator is half the resonance frequency of the QEPAS tuning fork (TF). A transimpedance amplifier connected to the TF is not shown. The *dashed line* indicates ultra-pure PFA (perfluoroalkoxy) tubing

4 Experimental results and discussion

For good performance, it is essential to optimize two QEPAS parameters, namely the sampled gas pressure and the laser current modulation depth [20, 22, 23]. For this sensor the optimum gas pressure inside the QEPAS cell was found to be 200 Torr, with a TF resonance frequency of $f = 32\,760$ Hz and a Q factor of 16 725. The optimum ICL current modulation amplitude at 200 Torr sample gas pressure was 4 mA, corresponding to 0.13 cm^{-1} and roughly matching ~ 2 times the collision-broadened FWHM (0.06 cm^{-1} at 200 Torr) of the selected absorption line, similar to the previous QEPAS studies [24]. The addition of 5% SF_6 to the N_2 diluting gas enhanced the QEPAS signal by a factor of two. Ambient air was also found to result in a factor of 1.5 higher QEPAS signal when it was used as a diluter in place of dry N_2. This effect is most likely due to its water content and the related increase of the V–T energy-transfer rate (the signal enhancement is not due to H_2O absorption, as this is one order of magnitude lower than that of H_2CO).

A spectral scan performed across the H_2CO absorption line at 2832.5 cm^{-1} (optimum selected line no. 2 as stated above in Sect. 2) at the above-mentioned experimental parameters is shown in Fig. 4. The H_2CO concentration was set to 17.7 ppmv and ambient air was employed as the diluting gas. The ICL frequency was scanned in 20-MHz steps. The lock-in time constant was 1 s with a 3-s delay between two consecutive measurements. The minimum detection sensitivity of the sensor was evaluated from the 1σ noise of the stepwise concentration measurements (see Fig. 5a) and was determined to be $2.2 \times 10^{-8}\,cm^{-1}\,W\,(Hz)^{-1/2}$ for an ICL power of 3.4 mW inside the cell (limited by the required spatial filtering of the applied laser beam and optical losses from the ZnSe lens and the sapphire windows of the QEPAS cell) and a peak formaldehyde absorbance of $6.6 \times 10^{-5}\,cm^{-1}$. This photoacoustic figure of merit is in reasonable agreement with the results

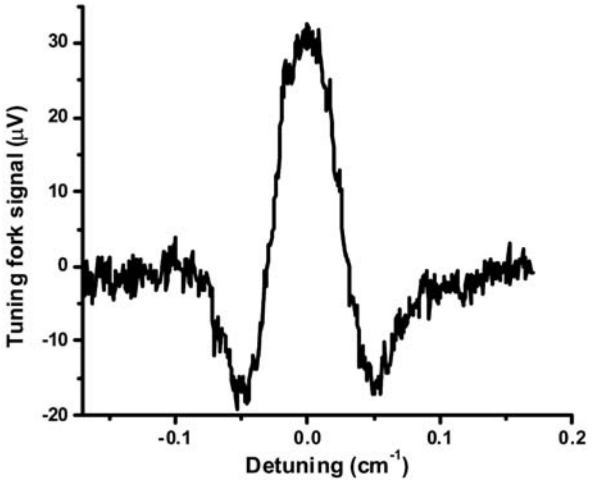

FIGURE 4 Second-harmonic QEPAS scan of the H_2CO absorption line at 2832.48 cm^{-1} (line no. 2 depicted in Fig. 2). The H_2CO concentration was 17.7 ppmv and the QEPAS cell pressure was 200 Torr. Ambient air was used as diluting gas

of recent near-infrared QEPAS-based trace-gas measurements [23].

Stepwise concentration measurements were performed to verify the linearity of the QEPAS signal as a function of the H_2CO concentration (see Fig. 5). The ICL was locked to the formaldehyde line at 2832.483 cm^{-1}. The gas standard generator was used to produce H_2CO concentrations in steps from 2 to 20 ppmv with ambient air as the diluting gas. The QEPAS signal for each concentration step was measured every 30 s for a total time duration of 10 min. The lock-in time constant was set to $\tau = 10$ s for these measurements. The results are depicted in Fig. 5a. Data for each step were averaged and a calibration curve was obtained (Fig. 5b) using the formaldehyde concentrations derived from the data sheets of the permeation tube. The results confirm that the QEPAS signal is proportional to the H_2CO concentration.

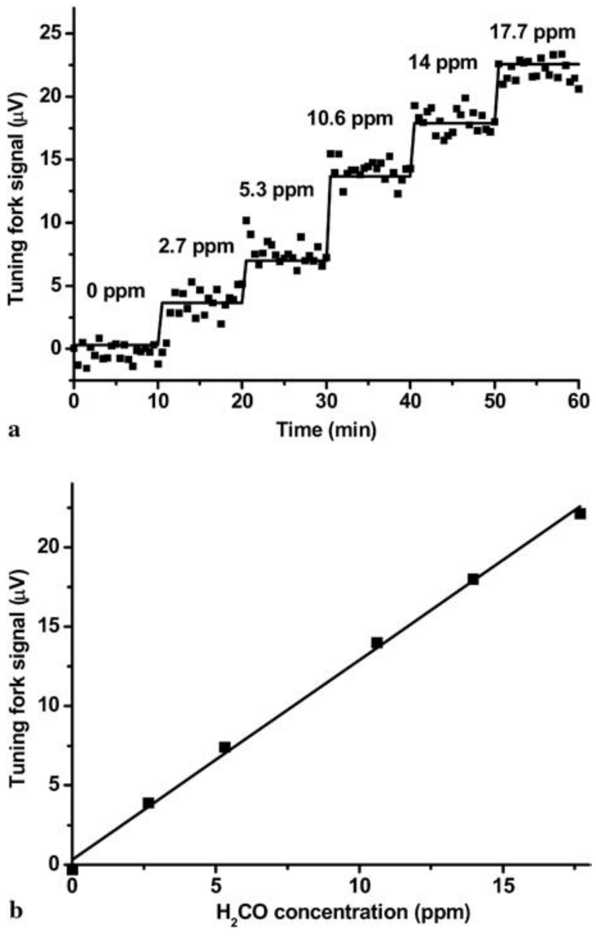

FIGURE 5 H_2CO monitoring for different concentrations in flow conditions. (**a**) Experimental data (*dots*) and calculated values (*line*). (**b**) Calibration curve obtained from measured QEPAS signals and known H_2CO concentration values from data supplied by permeation-tube vendor (KinTek)

The fundamental limit of the QEPAS-based spectrometer is determined by the thermal noise of the TF, which can be calculated theoretically [25] as

$$\frac{\sqrt{\langle V_{\mathrm{n}}^2 \rangle}}{\sqrt{\Delta f}} = R_{\mathrm{fb}} \sqrt{\frac{4 k_{\mathrm{B}} T}{R}}, \tag{1}$$

where $\sqrt{\langle V_{\mathrm{n}}^2 \rangle}$ is the RMS voltage noise observed at the transimpedance amplifier output (with a feedback resistor $R_{\mathrm{fb}} = 10\,\mathrm{M\Omega}$), Δf is the detection bandwidth, k_{B} is the Boltzmann constant, $T = 300$ K is the temperature, and $R = 68\,\mathrm{k\Omega}$ is the measured TF electrical resistance at the resonant frequency and 200 Torr gas pressure. If the lock-in amplifier time constant is τ, then $\Delta f = 1/\pi\tau$. The noise in one quadrature component is

$$\sqrt{\langle X_{\mathrm{n}}^2 \rangle} = \sqrt{\frac{\langle V_{\mathrm{n}}^2 \rangle}{2}}. \tag{2}$$

The noise calculated using (1) and (2) at the conditions corresponding to the measurements presented in Fig. 5 is $\sqrt{\langle X_{\mathrm{n}}^2 \rangle} = 0.62\,\mu\mathrm{V}$. The scatter of points in Fig. 5 gives $\sqrt{\langle X_{\mathrm{n}}^2 \rangle} = 0.68\,\mu\mathrm{V}$, which agrees with the theoretical thermal noise limit within the uncertainty of measurements. Thus, noise is not related to the laser radiation and therefore the detection limit is expected to be improved proportional to the laser power.

5 Conclusions

In summary, we have demonstrated the feasibility of using a novel cw 3.53-μm DFB ICL as a spectroscopic source for a QEPAS-based sensor to detect formaldehyde concentrations at sub-ppmv levels. The measured detection sensitivity of the sensor is $2.2 \times 10^{-8}\,\mathrm{cm^{-1}\,W\,(Hz)^{-1/2}}$, which is in agreement with other QEPAS-based gas analyzers [20, 23]. This detection sensitivity corresponds to 0.6 ppmv H_2CO concentration in air with 3.4 mW of laser power delivered to the QEPAS ADM and a time resolution of 10 s. It is expected that future ICL devices will be capable of emitting ∼ 100 mW or more optical power. Assuming that such ICL performance is achieved and all the emitted power is delivered to the ADM, the QEPAS-based H_2CO detection sensitivity would be ∼ 25 ppbv. Further gain in performance is anticipated with optimization of the microresonator design and by using lower-frequency TFs. Thus, the combination of a powerful thermoelectrically cooled ICL and a QEPAS ADM provides the technologies for compact field-deployable trace-gas sensors.

ACKNOWLEDGEMENTS The authors acknowledge B. Yang for device processing and R.E. Muller and P.M. Echternach for e-beam writing of DFB gratings. The authors gratefully acknowledge financial support from the National Aeronautics and Space Administration, the Texas Advanced Technology Program, the Robert Welch Foundation, and the Office of Naval Research via a subaward from Texas A&M University. A part of the research described in this publication was carried out at the Jet Propulsion Laboratory, California Institute of Technology, under a contract with the National Aeronautics and Space Administration. M. Horstjann acknowledges partial financial support from the Deutscher Akademischer Austauschdienst (DAAD), Bonn, Germany.

REFERENCES

1 R.Q. Yang: Superlattices Microstruct. **17**, 77 (1995)
2 R.Q. Yang, C.J. Hill, B.H. Yang, C.M. Wong, R.E. Muller, P.M. Echternach: Appl. Phys. Lett. **84**, 3699 (2004)
3 J.L. Bradshaw, N.P. Breznay, J.D. Bruno, J.M. Gomes, J.T. Pham, F.J. Towner, D.E. Wortman, R.L. Tober, C.J. Monroy, K.A. Olver: Physica E **20**, 479 (2004)
4 T. Aellen, S. Blaser, M. Beck, D. Hofstetter, J. Faist, E. Gini: Appl. Phys. Lett. **83**, 1929 (2003)
5 J.S. Yu, A. Evans, J. David, L. Doris, S. Slivken, M. Razeghi: IEEE Photon. Technol. Lett. **16**, 747 (2004)
6 http:// www.osha.gov / SLTC / formaldehyde / index.html
7 Committee on Toxicology, National Research Council: *Spacecraft Maximum Allowable Concentrations for Selected Airborne Contaminants, Vol. 1* (National Academy Press, Washington, DC 1994)
8 S.E. Ebeler, A.J. Clifford, T. Shibamoto: J. Chromatogr. B **702**, 211 (1997)
9 B.P. Wert, A. Fried, A.S. Rauenbuehler, J. Walega, B. Henry: J. Geophys. Res. **108**, 4350 (2003)
10 National Research Council: *Rethinking the Ozone Problem in Urban and Urban Regional Air Pollution* (National Academy Press, Washington, DC 1991)
11 Y. Suzuki, N. Nakano, K. Suzuki: Environ. Sci. Technol. **37**, 5695 (2003)
12 J.R. Hopkins, T. Still, S. Al-Haider, I.R. Fisher, A.C. Lewis, P.W. Seakins: Atmos. Environ. **37**, 2557 (2003)
13 J. Chen, S. So, H.S. Lee, M.P. Fraser, R.F. Curl, T. Harman, F.K. Tittel: Appl. Spectrosc. **58**, 243 (2004)
14 D. Richter, A. Fried, B.P. Wert, J.G. Walega, F.K. Tittel: Appl. Phys. B **75**, 281 (2002)
15 D. Rehle, D. Leleux, M. Erdelyi, F.K. Tittel, M. Fraser, S. Friedfeld: Appl. Phys. B **72**, 947 (2001)
16 H. Dahnke, G. von Basum, K. Kleinermanns, P. Hering, M. Murtz: Appl. Phys. B **75**, 311 (2002)
17 F. Muller, A. Popp, F. Kuhnemann, S. Schiller: Opt. Express **11**, 2820 (2003)
18 M.M.J.W. van Herpen, S.E. Bisson, A.K.Y. Ngai, F.J.M. Harren: Appl. Phys. B **78**, 281 (2004)
19 I.T. Sorokina: 'Crystalline Mid-infrared Lasers'. In: *Solid-state Mid-infrared Laser Sources*, ed. by I.T. Sorokina, K.L. Vodopyanov (Top. Appl. Phys. **89**) (Springer-Verlag Berlin Heidelberg 2003) pp. 255–349
20 A.A. Kosterev, Y.A. Bakhirkin, R.F. Curl, F.K. Tittel: Opt. Lett. **27**, 1902 (2002)
21 L.E. Christensen, C.R. Webster: JPL Intern. Rep. (2004)
22 A.A. Kosterev, Y.A. Bakhirkin, F.K. Tittel, S. Blaser, Y. Bonetti, L. Hvozdara: Appl. Phys. B **78**, 673 (2004)
23 D. Weidmann, A.A. Kosterev, F.K. Tittel: Opt. Lett. **29**, 1837 (2004)
24 A.A. Kosterev, F.K. Tittel: 'Ammonia detection using quartz-enhanced photoacoustic spectroscopy with a near-IR telecommunication diode laser', Appl. Opt. (2004), Vol. 43, accepted
25 R.D. Grober, J. Acimovic, J. Schuck, D. Hessman, P.J. Kindlemann, J. Hespanha, A.S. Morse, K. Karrai, I. Tiemann, S. Manus: Rev. Sci. Instrum. **71**, 2776 (2000)